VNU Journal of Science:
Computer Science and Communication Engineering

Journal homepage: http://www.jcsce.vnu.edu.vn/index.php/jcsce

Original Article

Hybrid Photonic–Electronic Inception CNNs with Nonlinear APMR Convolutions*

Thanh Tien Do[1], Trung Thanh Le[2]*

[1] *International School, Vietnam National University, 144 Xuan Thuy, Cau Giay, Hanoi, Vietnam*
[2] *Phenikaa School of Computing, Phenikaa University, Nguyen Trac, Duong Noi, Hanoi, Vietnam*

Received 29th January 2026
Revised 15th April 2026; Accepted 18th May 2026

Abstract: This paper introduces a novel, hybrid Inception CNN that uses all-pass microring resonators (APMRs) to perform optical convolution and nonlinear activation. The APMR-Inception module combines an optical branch with electronic branches to keep the model compact while still capturing multi-scale features. Experiments show stable training and good accuracy: around 85% on CIFAR-10, 95.2% on SVHN, and 62% on CIFAR-100. The model works well on structured objects and remains balanced performance across classes. Because many operations are done through passive optical interference, the system could reduce energy use and latency. Overall, the results indicate that nonlinear APMR-based photonic modules are a promising approach for building efficient deep learning models.

Keywords: All-pass microring resonator (APMR), Photonic neural networks, Hybrid optical–electronic CNN, Energy-efficient optical computing.

1. Introduction

Deep learning has become an essential component of modern computer vision and pattern recognition. When neural models grow larger and more complex, their computational and energy demands rise, particularly in convolutional neural networks (CNNs). While electronic hardware such as GPUs continues to advance, it faces fundamental limits in memory bandwidth and power efficiency. These constraints have triggered the research community to explore photonic computing as an alternative for high-speed and energy-efficient neural processing.

Optical neural networks (ONNs) offer several intrinsic advantages that address these bottlenecks. They can process information at high speed and consume much less energy, while also enabling natural parallelism because of the ability of light to propagate via multiple channels simultaneously. These benefits are recognized in prior studies. For example, one

*Corresponding author.
E-mail address: thanh.letrung@phenikaa-uni.edu.vn

https://doi.org/10.25073/2588-1086/vnucsce.6886

work highlights that optical signal processing has special strengths such as high speed, low energy use, and strong parallelism [1]. Likewise, another study indicates that optical systems provide parallelism, high bandwidth, low energy consumption, and minimal delay [2]. Recent reviews reinforce these observations: optical devices allow ultralarge bandwidth and ultralow power consumption, and optical matrix operations can increase computing speed by several orders of magnitude [3]. Additionally, the inherent advantages of optics—including high-speed performance, energy efficiency, and parallel information processing—are further emphasized in integrated photonic neuromorphic platforms [4].

These properties make ONNs suitable for accelerating convolution operations, which dominate the computational cost of CNNs. As noted in an optical Fourier CNN study, the convolution step becomes expensive and demands significant electronic resources when image resolution increases [5]. Furthermore, optical CNN reviews highlight that photonic convolution can improve computing speed and reduce power when compared to electronic vector–matrix multiplication [3].

Despite these promising characteristics, many existing optical CNN designs continue to rely on electronic hardware for nonlinear activation. This reliance can limit overall system efficiency because it introduces electronic overhead into what is otherwise an optical pipeline. For instance, one review observes that nonlinear activation is still performed in the camera and electrical domain [6]. The same review further explains that nonlinear functions and fully connected layers are typically retained in the electronic domain in most implementations [6]. Additionally, a 2021 ONN survey reports that several optical systems still lack integrated nonlinear activation, which prevents them from achieving fully optical learning architectures [7]. More recent studies confirm that ONNs still rely on electronic nonlinear activation, thereby decreasing their potential performance [8].Recent studies indicate that this limitation is fundamentally related to the analog nature of ONNs, where conventional digital activation designs are not fully compatible [9] , while practical optical nonlinear mechanisms is still limited [10]. As a result, many systems still rely on opto-electronic conversions for nonlinear processing, increasing latency and energy consumption, and hindering fully optical implementations [11]. Furthermore, electro-photonic neural network research suggests that the absence of efficient optical activation limits development of multilayer photonic architectures [12].

To address these limitations, researchers have investigated microring resonators as compact and efficient nonlinear elements. These devices can create strong nonlinear responses while remaining a small footprint, making them more practical for integration into large photonic circuits. Nanophotonic neural networks offer advantages for efficient optical processing; optical signals can be processed without additional energy, and linear optical networks can operate at the speed of light with minimal power consumption [13]. Furthermore, optical convolution and matrix multiplication have been successfully demonstrated in integrated non-spiking photonic circuits, underscoring the feasibility of photonic computation [14]. Hybrid ONN research also demonstrates that photonic accelerators could enhance energy efficiency by offloading convolution layers from electronic processors [15].

To overcome the gap—namely, the lack of integrated nonlinear optical activation—we introduce a hybrid architecture called APMR-Inception, in which nonlinear all-pass microring resonators (APMRs) perform both optical convolution and activation inside the Inception module. The APMR node utilizes cascaded microrings, where the output intensity serves

as a nonlinear activation function, enabling the optical branch to replace the standard 3×3 convolution with a compact, nonlinear photonic alternative. By combining APMR-based nonlinear convolution with lightweight electronic branches, the hybrid system can extract multi-scale features more efficiently, which reduces energy consumption and improves latency.

Unlike existing hybrid optical–electronic neural networks, which rely on optical computation for linear operations while retaining nonlinear activation in the electronic domain, the proposed APMR-Inception architecture introduces a fundamentally different design paradigm. In our approach, the all-pass microring resonator (APMR) simultaneously performs convolution and nonlinear activation within a single optical unit through its intrinsic intensity response. This eliminates the need for separate activation layers and reduces optical–electrical conversion overhead. Furthermore, the proposed method embeds nonlinear optical computation directly into a multi-branch Inception structure, enabling efficient multi-scale feature extraction while maintaining hardware efficiency.

This work makes several key contributions to the development of nonlinear photonic neural architectures:

Nonlinear optical Inception module: We present APMR-Inception, where all-pass microring resonators implement both convolution and nonlinear activation in the optical domain.

Hybrid optical–electronic processing: The module combines an APMR optical branch with lightweight electronic paths for multi-scale feature extraction.

Practical evaluation: Integrated into a full network, APMR-Inception achieves competitive accuracy with lower computational overhead, offering a step to deeper optical neural systems.

2. Proposed Architecture: APMR-Inception

2.1. Theoretical Model of APMR Node

All-Pass Microring Resonators (APMRs) offer a compact and energy-efficient way in order to realize nonlinear optical transfer functions inside photonic neural networks. A single APMR ring, defined by its self-coupling coefficient a, round-trip attenuation t, and round-trip phase shift ϕ, has a normalized power transmission described in [16] as:

$$H(\phi) = \left| \frac{t - ae^{i\phi}}{1 - tae^{i\phi}} \right|^2 \tag{1}$$

where the phase term

$$\phi = \frac{2\pi n_{\text{eff}} L}{\lambda} + \Delta\phi \tag{2}$$

depends on the effective refractive index n_{eff}, the ring circumference L, and an electrically induced phase shift $\Delta\phi$. The squared magnitude highlights that the photodetector responds to optical intensity, rather than the field amplitude itself.

In our proposed APMR node, three microring resonators are cascaded, and each ring contains three phase shifters (Figure 1). These phase shifters are driven by electrical signals proportional to $x \cdot w$, where x is the image pixel value, and w is a trainable weight. This relationship is implemented as a linear gain at the driver or DAC, which adjusts the voltage before reaching the phase shifter. As a result, the phase modulation remains dependent on both the input data and the learned weight. In addition, the use of three phase shifters per microring is also aligned with the structure of the 3×3 convolution operation. In the proposed architecture, each APMR unit replaces a 3×3 convolution kernel. The three-phase shifters provide a compact representation of multiple kernel weights by mapping input–weight interactions into phase modulation. Although this mapping is not one-to-one with all nine kernel elements, it allows

for an efficient convolutional operation while remaining low in hardware complexity.

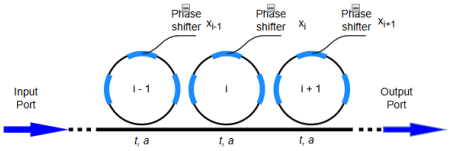

Figure 1. APMR node with cascaded microring.

The combined optical field after passing through the three APMRs is:

$$E_{\text{out}} = E_{\text{in}} \cdot \prod_{k=1}^{3} H_k(\phi_{k,1}, \phi_{k,2}, \phi_{k,3}) \qquad (3)$$

where H_k represents the transfer function of the k-th ring with its three independent phase-shifter inputs. The photodetector then measures the output intensity:

$$I_{\text{out}} = |E_{\text{out}}|^2 \qquad (4)$$

which functions as the nonlinear activation of the photonic neuron. In this model, the input intensity is normalized to 1, which ensures scaling throughout training and inference. This formulation enables a nonlinear mapping, which is essential for high-capacity CNN deep learning architectures such as Inception and VGGs.

2.2. *Hybrid Optical–Electronic Inception Architecture*

In our workflow, the optical behaviour of the APMR rings is first examined using FDTD simulation, and the resulting parameters are then integrated into a Python-based implementation on Google Colab Pro for network training and evaluation.

The APMR-Inception architecture uses electronic convolutional processing and nonlinear optical computation, that forms a hybrid system designed to accelerate multi-branch feature extraction. The model integrates all-pass microring resonator (APMR) layers into an Inception-style CNN. The 3×3 and enlarged receptive-field branches are implemented optically using cascaded APMR units, while the 1×1 and pooling branches remain electronic. In the core of each optical branch, an APMRConv2d module replaces the standard 3×3 convolution with three cascaded microring resonators, each controlled by thermo-optic phase shifters that encode the learnable weights. This nonlinear intensity response enables the optical domain to perform both filtering and activation in a single physical step, complementing the lighter electronic branches.

To support this hybrid design on a silicon-on-insulator platform, the system uses a wavelength-division multiplexing (WDM) network, combining multiple on-chip laser wavelengths and distributing them to the APMR nodes via standard multiplexing components. After typical routing losses, each node receives optical power for stable operation, and optical amplifiers may be added when scaling to larger arrays. Within each optical branch, the output of the cascaded rings is directed to a balanced photodetector pair. These signals are then amplified and digitized, allowing the optical outputs to be synchronized and merged with the electronic branches during concatenation in the Inception block.

To reduce instantaneous hardware load, feature channels can be divided into several groups and processed in separate time slots under fast electronic or optical control. Only a subset of APMR nodes is active at any moment, yet the latency remains low because of rapid configuration and readout. Importantly, the spatial outputs and multi-branch structure of the Inception module are preserved at the network level, ensuring that the hybrid optical–electronic system maintains the same functional behaviour as its software counterpart while benefiting from the efficiency of nonlinear photonic computation.

3. Experimental Evaluation and Discussion

3.1. APMR-Inception Configuration

The overall architecture of the APMR-Inception-Tiny is illustrated in Figure 2. The workflows follows a hierarchical multi-stage design that integrates electronic and photonic computation within an Inception-style framework.

The model takes a 32×32×3 CIFAR-10 input and begins with a 3×3 convolutional stem layer that expands the feature dimension into 32 channels. This is followed by three Inception stages, where each stage includes multi-branch modules combining electronic and APMR-based photonic operations.

Inception Stage 3 contains two blocks, Inception-3a and Inception-3b. As shown in Figure 2 , Inception-3a expands the feature dimension from 32 to 96 channels using four parallel branches. Branch 1 implemenst a standard 1×1 convolution, while Branch 4 imlements max pooling followed by a 1×1 convolution, both implemented in the electronic domain. In contrast, Branch 2 and Branch 3 present photonic computation, where standard 3×3 convolutions are used by APMRConv layers. In particular, Branch 3 uses two cascaded APMRConv layers to increase nonlinear expressiveness. The outputs of all branches are concatenated to form the final feature representation.

Inception-3b follows the same multi-branch structure and further increases the feature dimension from 96 to 128 channels. A 2×2 max-pooling operation then reduces the spatial resolution from 32×32 to 16×16.

Inception Stage 4 and **Stage 5** follow the same structural pattern in Stage 3. Instead of redefining the configuration of the branch, these stages expand the channel dimensions to increase representational capacity. Stage 4 consists of two Inception blocks (128→144 and 144→192), followed by a 2×2 max pooling layer that reduces the feature map to 8×8. Stage 5 contains a final Inception module (192→256) with the same hybrid branch structure.

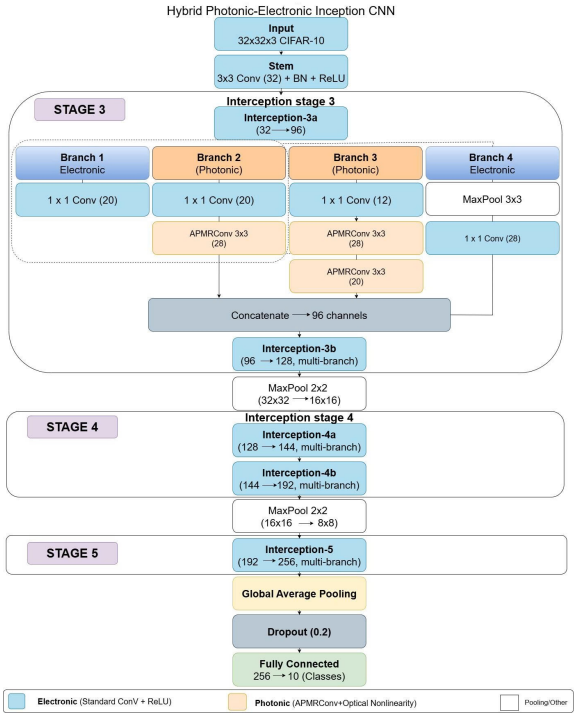

Figure 2. Architecture of the proposed APMR-Inception-Tiny.

At the network head, global average pooling is applied to aggregate spatial features, followed by a dropout layer (0.2) and a fully connected classifier that maps the 256-dimensional feature vector to 10 output classes.

As highlighted in Figure 2, a key design characteristic of the proposed architecture is the hybrid computation scheme. Electronic branches (blue) implement lightweight linear operations, while photonic branches (orange) implement both convolution and nonlinear activation via cascaded APMR units. This design allows for multi-scale feature extraction while embedding nonlinear optical computation into the network.

3.2. Training Behaviour and Evaluation Results

The model is trained on the CIFAR-10 dataset, which uses the standard 50,000/10,000 train–test split. Inputs are augmented with random cropping and horizontal flipping before being normalized. Training is performed for 100 epochs using AdamW (learning rate 1×10^{-3}, weight decay 1×10^{-4}), cosine learning-rate scheduling, gradient clipping (1.0), and label smoothing (0.05).

Figures 3 and 4 show stable and smooth convergence. Training accuracy approaches 89%, while the accuracy of test stabilises around 84–85%. Both training and test losses go down consistently without sharp fluctuations that indicate stable regularisation and good stability of the hybrid optical–electronic architecture.

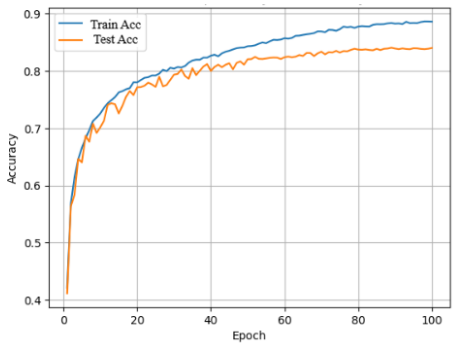

Figure 3. Train and test accuracy on CIFAR-10.

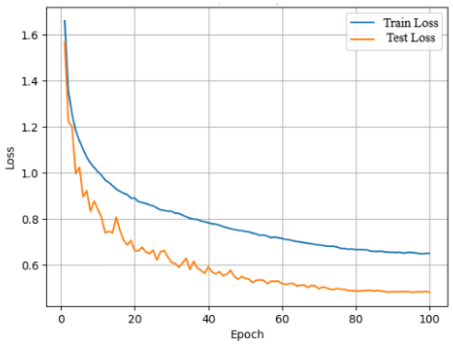

Figure 4. Train and test loss on CIFAR-10.

Sample predictions in Figure 5 demonstrate that the model recognizes a wide range of images correctly, even when objects appear in cluttered scenes or unusual poses. Misclassifications mainly arise in ambiguous cases, such as animals with similar textures or colours.

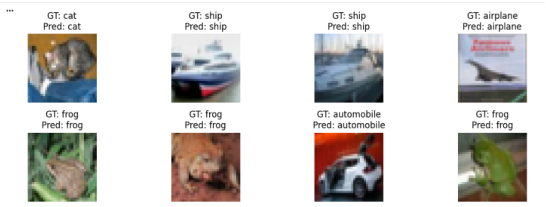

Figure 5. Sample predictions on CIFAR-10.

3.3. Class-Level Performance

The per-class accuracy plot reveals that performance is relatively balanced across the dataset. Vehicle and high-texture categories such as automobile, ship, and truck achieve the highest accuracies (92.3%, 90.7%, and 91.3% respectively). More challenging animal classes such as cat (70.3%) and dog (78.1%) show lower scores, which aligns with their higher intra-class variation and overlapping textures.

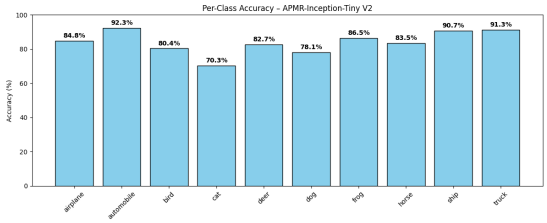

Figure 6. Per-class accuracy on CIFAR-10.

The confusion matrix (see Figure 7) highlights the same trend: misclassifications mostly occur among semantically similar animal categories (e.g., cat ↔ dog, bird ↔ deer), while vehicle-related classes show clear separation, with strong diagonals and fewer cross-category errors. This indicates that the hybrid optical–electronic feature extraction

pipeline is particularly effective for structured shapes and edges.

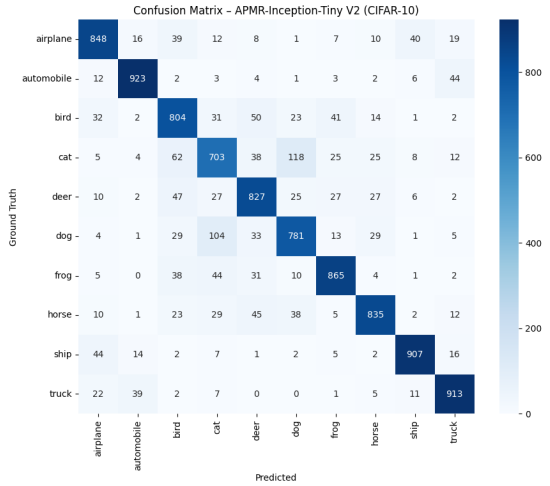

Figure 7. Confusion matrix on CIFAR-10.

3.4. *Cross-Dataset Robustness on SVHN and CIFAR-100*

To evaluate robustness in different complext datasets, we re-train APMR-Inception-Tiny on the SVHN digit dataset, which contains 73,257 training and 26,032 test images with very different statistics from CIFAR-10. Apart from adapting input normalisation, all architectural and training settings are kept almost similar.

As shown in Figures 8 and 9, the model converges quickly and smoothly: test accuracy exceeds 88% within ten epochs and reaches 95.2%, with a test loss of about 0.20 and only a small gap to the training curve.

Also, we test the same configuration on CIFAR-100 and obtain a top-1 accuracy of 62%. This score is slightly lower than that of electronic CNNs with similar depth and width on the same dataset, but the hybrid photonic–electronic design offers a clear advantage in energy efficiency and has the potential to reduce latency and power consumption when deployed on-chip.

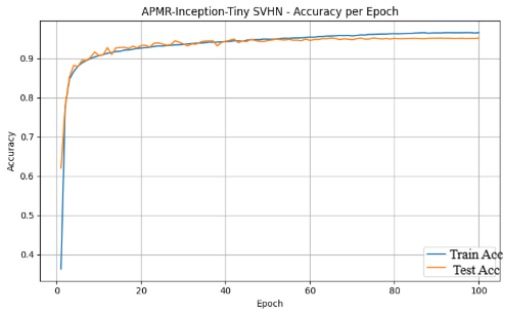

Figure 8. The accuracy on SVHN dataset.

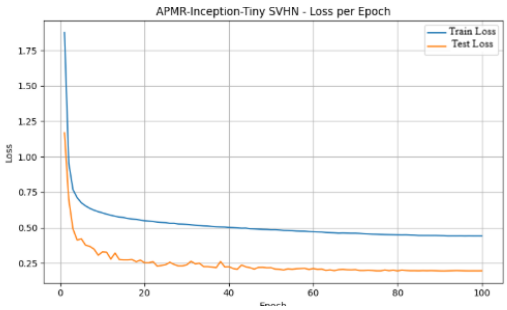

Figure 9. The loss on SVHN dataset.

3.5. *Energy Analysis of the Optical Branches*

For one optical output, the total energy can be estimated as:

$$E_{\text{opt-branch}} = E_{\text{laser}} + E_{\text{WDM/routing}} + E_{\text{APMR}} + E_{\text{PD/TIA}} + E_{\text{ADC}} + E_{\text{DAC/driver}} + E_{\text{OA}} \quad (5)$$

This includes the optical source, routing loss, APMR processing, photodetection, and electrical readout.

Based on typical values in photonic systems, the optical signal energy is around 1–3 pJ per output. The photodetector, amplifier, and ADC add about 3–15 pJ. Therefore, the total energy of one optical 3×3 output is about 5–20 pJ in the normal inference case. In a more conservative case, when phase reconfiguration is frequent, the energy can increase to 15–50 pJ.

In comparison (Table 1), a standard electronic 3×3 convolution requires 9 multiply-accumulate (MAC) operations. Each MAC consumes about 4–5 pJ, so the total is already about 40–45 pJ,

without counting memory access and activation. In practice, the total energy is often 50–80 pJ per output.

This shows that the proposed optical branch can reduce energy by about 2.5× to 10× in favorable conditions. The main reason is that the APMR performs convolution and nonlinear response in one physical step, while electronic systems require multiple operations and memory access.

3.6. Comparison with Electronic Inception Baseline

To investigate the effectiveness of the model, we compare APMR-Inception-Tiny with a electronic Inception-Tiny model in the same, identical topology. The electronic baseline achieves a higher accuracy on CIFAR-10 (≈ 90.4%), compared to ≈ 85% for the APMR-based model. This gap is due to the constrained nonlinear behavior of the APMR transfer function and the absence of fully flexible digital activation functions.

However, the APMR-Inception model offers a key advantage. In electronic CNNs, convolution and activation are implemented as separate operations, which requires multiple memory accesses and computational steps. In contrast, the APMR node performs both operations simultaneously via the nonlinear optical transfer function.

In terms of training time, both models are implemented in simulation and show similar convergence behavior, as illustrated in Figures 2 and 3. The additional computational cost of evaluating the APMR transfer function is quite small. In terms of inference, the electronic model relies on sequential multiply-accumulate operations, while the APMR-based model can perform convolution and activation in a single optical propagation step. This show that, when implemented in hardware, the APMR-Inception architecture could achieve lower latency and reduced energy consumption.

Therefore, the proposed model trades some accuracy for a more hardware-efficient computation paradigm, adapting for future photonic neural network implementations.

3.7. Overall Performance and Discussion

Across 100 epochs, APMR-Inception-Tiny shows reliable behaviour. The model achieves test accuracy of around 85% on CIFAR-10 while using a very small number of parameters, showing that nonlinear APMR-based convolutions can extract strong features without increasing model size. Training curves remain smooth, supported by the optical nonlinearity and label smoothing. The per-class results indicate balanced performance: most categories are recognised well, with predictable drops in animal classes, while structured objects reach higher scores due to the multi-branch Inception design.

Cross-dataset experiments further confirm this trend. On SVHN, the model achieves 95.2%, showing that the architecture generalises extremely well to data with different visual patterns. On CIFAR-100, the model reaches 62%, which is slightly lower than electronic CNNs in the similar size. However, the hybrid structure still offers a clear advantage in potential hardware efficiency.

One important benefit of the proposed model is its energy-saving potential when implemented on photonic hardware. Many MAC operations in the APMR branches are deployed via passive optical interference rather than electronic multiplications. This reduces the demand for frequent memory access and avoids the high switching costs which are associated with transistor-based MAC units. Together with wavelength-division multiplexing and passive microring propagation, multiple channels can be processed at the same time using only a small amount of optical power. As a result, the architecture is expected to reach lower energy per operation and reduced overall power

Table 1. branch-level energy comparison for one 3×3 output

Component	Optical 3×3 branch	Electronic 3×3 branch
Optical source / launched signal	1–3 pJ	—
WDM + routing overhead	included	—
Balanced PD + TIA	2–14 pJ	—
ADC	1–2 pJ	—
DAC / phase-driver overhead	amortized	—
9 MAC operations	—	≈41.4 pJ
Separate activation	intrinsic	additional
Memory / data movement	reduced	10+ pJ
Total energy	**5–20 pJ (amortized), 15–50 pJ**	**50–80 pJ**

consumption compared with an all-electronic model that provides similar accuracy.

Regarding latency, optical computation offers reduced delay due to its inherent parallelism and the fact that convolution and nonlinear response are performed within a single optical propagation step. In contrast, conventional electronic implementations rely on sequential multiply-accumulate operations and separate activation stages. Therefore, the proposed architecture provides a latency advantage at the architectural level, rather than a guaranteed reduction under all hardware conditions.

Finally, these results have shown that combining APMR-based optical computation with an Inception-style design advances feature diversity while maintaining a low computational cost. This enables APMR-Inception-Tiny to be a promising direction for lightweight and energy-efficient photonic-assisted deep learning models.

4. Conclusions

This work introduced a hybrid Inception-style CNN that integrates nonlinear all-pass microring resonators into key convolution branches to improve efficiency and feature extraction capacity. The proposed APMR-Inception-Tiny model showed stable training behaviour and maintained strong accuracy despite its compact size. It delivered good performance on CIFAR-10, generalised well to SVHN, and achieved reasonable results on CIFAR-100. The nonlinear response of the APMR units helped the optical branches capture richer features without increasing computational cost. Because many operations are performed optically via passive interference, the architecture has clear potential to reduce power consumption and enable faster inference on photonic hardware. Overall, the study demonstrates that combining photonic nonlinear computation with Inception-style design is a promising approach for future energy-efficient deep learning systems.

CRediT authorship contribution statement. Thanh Tien Do: Conceptualization, Methodology, Software, Investigation, Formal analysis, Writing – original draft, Visualization. Trung Thanh Le: Validation, Formal analysis, Writing – review & editing, Supervision.

Declaration of competing interest. The authors declare that they have no known competing financial interests or personal relationships that could have appeared to influence the work reported in this paper.

References

[1] W. Yu, S. Zheng, Z. Zhao, B. Wang, W. Zhang - Reconfigurable Low-Threshold All-Optical Nonlinear Activation Functions Based on an Add-Drop Silicon Microring Resonator. IEEE Photonics Journal, 14 (2022) 1–7, https://doi.org/10.1109/jphot.2022.3219246

[2] S. Amiri, M. Miri - All-Optical Convolutional Neural Network Based on Phase Change Materials in Silicon Photonics Platform. Scientific Reports, 15 (2025) 22055, https://doi.org/10.1038/s41598-025-06259-4

[3] Z. Tao, H. Ouyang, Q. Yan, S. Du, H. Hao, J. Zhang, J. You - On-Chip Photonic Convolutional Processing Lights Up Fourier Neural Operator. MDPI, (2025), https://doi.org/10.3390/photonics12030253.

[4] A. Skalli, S. Sunada, M. Goldmann, M. Gebski, S. Reitzenstein, J. A. Lott, T. Czyszanowski, D. Brunner - Model-Free Front-to-End Training of a Large High-Performance Laser Neural Network. arXiv Preprint arXiv:2503.16943, (2025).

[5] Y. Liu, J. Qin, Y. Liu, Y. Liu, X. Liu, F. Ye, W. Li - Optical Fourier Convolutional Neural Network with High Efficiency in Image Classification. Optics Express, 32 (2024) 23575–23583, https://doi.org/10.1364/oe.522842

[6] X. Meng, N. Shi, G. Li, W. Li, N. Zhu, M. Li - Optical Convolutional Neural Networks: Methodology and Advances. Applied Sciences, 13 (2023) 7523.

[7] J. Liu, Q. Wu, X. Sui, Q. Chen, G. Gu, L. Wang, S. Li - Research Progress in Optical Neural Networks: Theory, Applications and Developments. PhotoniX, 2 (2021) 5, https://doi.org/10.1186/s43074-021-00026-0

[8] C. Zhu, T. Wang, P. L. McMahon, D. Soh - Quantum Optical Neural Networks Using Atom-Cavity Interactions to Provide All-Optical Nonlinearity. arXiv Preprint arXiv:2511.06167, (2025).

[9] Z. Lu, J. Tao, X. Wang, J. Liu, L. Wang, S. Mei, J. Li - Optimizing Optical Neural Network Design for Enhanced Compatibility with Analog Computation. Optics Express, 33(2) (2025) 2499–2511, https://doi.org/10.1364/oe.550613

[10] J. Xi, R. S. Tanuwijaya, T. Li, J. Li - Optical Neural Networks with Intensity-Based Projection Layers as Effective Nonlinear Activations. Scientific Reports, (2025), https://doi.org/10.1038/s41598-025-30632-y.

[11] S. Xiang, Y. Chen, H. Zhao, S. Shi, X. Zeng, Y. Zhang, Y. Hao - Nonlinear Photonic Neuromorphic Chips for Spiking Reinforcement Learning. Optica, 13(3) (2026) 457–468, https://doi.org/10.1364/optica.578687.

[12] G. Cong, N. Yamamoto, R. Kou, Y. Maegami, S. Namiki, K. Yamada - Vertically Hierarchical Electro-Photonic Neural Network by Cascading Element-Wise Multiplication. APL Photonics, 9 (2024), https://doi.org/10.1063/5.0197033.

[13] K. Demertzis, G. Papadopoulos, L. Iliadis, L. Magafas - A Comprehensive Survey on Nanophotonics Neural Networks. arXiv Preprint arXiv:2111.01550, (2021).

[14] L. El Srouji, Y.-J. Lee, M. B. On, L. Zhang, S. B. Yoo - Scalable Nanophotonic-Electronic Spiking Neural Networks. IEEE Journal of Selected Topics in Quantum Electronics, 29 (2022) 1–13, https://doi.org/10.1109/jstqe.2022.3217011.

[15] J. Gene, S. Park, H. C. Shin, J. M. Sohn - Optical Convolutional Neural Network with the Hybrid Training Method. Neurocomputing, (2025) 132080, https://doi.org/10.1016/j.neucom.2025.132080.

[16] V. Van - Optical Microring Resonators: Theory, Techniques, and Applications. CRC Press, (2016).